HOXA11-OS participates in lupus nephritis by targeting miR-124-3p mediating Cyr61 to regulate podocyte autophagy

Xiuhong Pan
Youjiang Medical University for Nationalities
Shanshan Chen
Youjiang Medical University for Nationalities
Ruiwen Shen
Youjiang Medical University for Nationalities
Sen Liu
Youjiang Medical University for Nationalities
Yanwu You (youyanwu1@163.com)
People's Hospital of Guangxi Zhuang Autonomous Region https://orcid.org/0000-0001-8162-8948

Research Article

Keywords: HOXA11-OS, Autophagy, Lupus nephritis, Cyr61, miR-124-3p

Posted Date: July 20th, 2022

DOI: https://doi.org/10.21203/rs.3.rs-1658735/v1

Abstract

Background: The long chain non-coding RNA HOXA11-OS was recently identified. Increasing studies have shown that HOXA11-OS has regulatory effects on genes in gastric cancer, prostate cancer, and various kidney diseases, but research on its role in systemic lupus erythematosus is still lacking. The present study aimed to investigate the role of HOXA11-OS in the regulation of podocyte autophagy in the development of lupus nephritis (LN) and its potential molecular mechanism.

Methods: mRNA and protein expression levels of the target gene (i.e., Cyr61) were detected by quantitative real-time polymerase chain reaction, western blotting, and immunofluorescence. Mouse podocytes were induced using serum immunoglobulin G (IgG) from patients with lupus and their viability was detected using the cell counting kit-8 assay. The interaction of miR-124-3p with HOXA11-OS and Cyr61 was analyzed by double luciferase reporter gene assay. Serum autoantibody levels were detected by enzyme-linked immunosorbent assay. Pathological lesions in kidney tissue were detected by hematoxylin-eosin and periodate Schiff staining. The independent samples *t*-test was used for comparing two groups, and one-way analysis of variance for comparing multiple groups.

Results: HOXA11-OS was highly expressed in LN tissues, serum, and cells, and the expression levels of some key autophagy factors and Cyr61 were significantly increased, while miR-124-3p was significantly decreased. In vitro, LN-IgG inhibited podocyte activity, increased autophagy and Cyr61 expression, and aggravated podocyte injury in a time and dose dependent manner. As a competitive endogenous RNA of miR-124-3p, HOXA11-OS promoted the expression of Cyr61, thus enhancing the autophagy increase induced by LN-IgG and aggravating podocyte injury. Knockdown of HOXA11-OS had the opposite effect. miR-124-3p mimic or Cyr61 knockdown restored the high expression levels of autophagy factors and Cyr61 induced by HOXA11-OS overexpression, and alleviated podocyte injury. Further in vivo experiments showed that injection of sh-HOXA11-OS adeno-associated virus downregulated HOXA11-OS and significantly alleviated renal damage in lupus mice.

Conclusions: HOXA11-OS is involved in the occurrence and development of LN by regulating podocyte autophagy through miR-124-3p/Cyr61 sponging, which may provide a good potential therapeutic target for LN.

Background

Lupus nephritis (LN) is a kind of glomerulonephritis and the most serious organ injury in systemic lupus erythematosus (SLE)[1]. Podocytes are highly differentiated epithelial cells in the kidney tissue that play a key role in maintaining the selective filtration of glomeruli[2, 3]. The podocyte marker proteins, nephrin and podocin, can form the hiatus septum complex, connect foot processes to form the hiatus septum, and prevent proteins and solutes from entering urine from circulation[4, 5]. Therefore, maintaining podocyte activity and structural integrity is very important for the clinical treatment of glomerular diseases and chronic kidney diseases.

The opposite strand of homeobox A11 (HOXA11-OS) is a common long non-coding RNA (lncRNA), which can compete with specific micro RNAs (miRNAs) as a competitive endogenous RNA (ceRNA), thus changing the expression of downstream key genes and participating in the occurrence and development of many diseases[6–8]. For example, HOXA11-OS can increase the expression of integrin β3 through sponging miRNA miR-124-3p, which can promote the migration and invasion of gastric cancer[9]. However, the mechanism of HOXA11-OS in SLE is still unknown. Therefore, we hypothesize that HOXA11-OS can target miR-124-3p regulatory factors to play a role in LN.

Cysteine rich 61 (Cyr61) is a recently identified secreting stromal cell protein existing at low level under steady state conditions, which can mediate various cell activities including cell survival, proliferation, differentiation, migration, adhesion, and synthesis of extracellular matrix[10]. It has been confirmed[11] that serum Cyr61 level is recognizably increased in SLE patients, which might be due to the increase of Cyr61 expressed in epithelial cells and released into blood through renal blood circulation. In addition, Cyr61 is closely related to clinical disease activity and inflammation of SLE. A recent study[12] has shown that during the inflammatory state Cyr61 is involved in the autophagy and apoptosis of renal tubular dermal cells. Autophagy is an intracellular degradation system that maintains cell homeostasis and integrity[13]. Programmed cell death-1 (Beclin-1) and microtubule associated protein 1 light chain 3 (LC3) are well-known and the most commonly used autophagy-related markers in the autophagy pathway[14, 15]. In LN, podocytes usually show abnormally high levels of structural autophagy[16, 17]. Therefore, autophagy might be involved in the complex occurrence and development of LN. However, autophagy abnormality is only the manifestation of podocyte injury, and the relationship between autophagy abnormality and podocyte injury is not completely clear thus requiring further research.

In the present study, HOXA11-OS was highly expressed in the kidney tissue and cells of lupus mice and in the blood of lupus patients. Overexpression of HOXA11-OS promoted the expression of Cyr61, thus enhancing the serum immunoglobulin G (IgG)-induced podocyte autophagy in lupus patients and aggravating podocyte injury. Knocking down HOXA11-OS showed the opposite. In addition, as a ceRNA, HOXA11-OS regulated the expression of Cyr61 by sponging miR-124-3p. Based on these results, we hypothesize that the HOXA11-OS/miR-124-3p/Cyr61 regulatory network may be involved in the occurrence and development of LN by regulating podocyte autophagy. Therefore, HOXA11-OS was further investigated to verify this hypothesis and propose a new LN treatment strategy.

Methods

Reagents

The lentivirus and adeno-associated virus (AAV) were constructed at Shanghai Jikai Gene Chemistry Technology Co. Ltd. (Shanghai, China). Primers were synthesized by Shanghai Shenggong Biotechnology Company (Shanghai, China). The enhanced chemiluminescence (ECL) kit, rabbit anti-glyceraldehyde 3-phosphate dehydrogenase (GAPDH) primary antibody (batch No.: 62u0922), rabbit anti-Cyr61 primary antibody (batch No.: 88x3333), mouse anti-tubulin primary antibody (batch No.: 6915213), goat anti-rabbit IgG secondary antibody (batch No.: 56j9958), and goat anti-mouse IgG secondary antibody (batch No.: 20000242) were purchased from Affinity Biosciences (Cincinnati, OH, USA). Rabbit anti-Beclin-1 primary antibody (batch No.: ab210498), rabbit anti-LC3B primary antibody (batch No.: ab192890), rabbit anti-nephrin primary antibody (batch No.: ab216341), and rabbit anti-podocin primary antibody (batch No.: ab181143) were obtained from Abcam (Cambridge, UK). Mouse anti-LC3B primary antibody (batch No.: K0420) was purchased from Santa Cruz Biotechnology Inc. (Dallas, TX, USA) and rabbit anti-β-actin primary antibody (batch No.: UD277186) from Invitrogen (Waltham, MA, USA). Goat anti-rabbit fluorescent antibody (batch No.: 211061011) and goat anti-mouse fluorescent antibody (batch No.: 216470915) were obtained from Beijing Zhongshan Jinqiao Biological Co. Ltd. (Beijing, China). The human IgG concentration detection kit (batch No.: TPFYJ7G4IY) was obtained from Elabscience Biotechnology Co. Ltd. (Houston, TX, USA). Enzyme-linked immunosorbent assay (ELISA) kits for mouse anti-double stranded DNA (dsDNA) antibody (batch No.: C05012542), mouse anti-nuclear antibody (ANA; batch No.: C05012540), and mouse anti-Smith (Sm) antibody (batch No.: C06012543) were purchased from CUSABIO Biotech Co. Ltd. (Houston, TX, USA). Cell Counting Kit-8 (CCK-8; batch No.: 20210828) was obtained from MCE (Suzhou, China) and the double luciferase detection kit (batch No.: E1910) from Beijing Promega Biotechnology Co. Ltd. (Beijing, China).

Sample collection from patients

Serum samples were collected from 20 patients with diagnosed LN hospitalized in the Department of Nephrology and Immunology of Affiliated Hospital of Youjiang Medical College for Nationalities from July 2020 to August 2021. Sera from ten healthy people were collected as control samples. All participants signed informed consent forms. The collected serum samples were approved by the Ethics Committee of the Affiliated Hospital of Youjiang Medical College for Nationalities. The samples were used to detect the expression levels of HOXA11-OS, Cyr61, Beclin-1, and LC3B, and to extract and purify IgG.

Animal experiments

Four-month-old C57BL/6J female mice and MRL/lpr female mice were purchased from Jiangsu Changzhou Cavens Experimental Animal Co. Ltd. (License No.: SCXK (Su) 2016-0010; Changzhou, China). The mice were raised in the animal room of the Experimental Animal Center of Youjiang Medical College for Nationalities in a specific-pathogen-free(SPF) environment. SPF laboratory was a 12h/12h alternating light and dark barrier system, ambient temperature: 22-24℃, relative humidity: 60-70%. Animal experiments were approved by the Ethics Committee of Youjiang Medical College for Nationalities (Approval No.: 2020043001), and all procedures were carried out according to the guidelines of the National Institute of Health. All the experimental operations were carried out under anesthesia to alleviate the pain of experimental animals as much as possible.

Adeno-associated virus used in mouse kidney orthotopic injection was designed and constructed by Shanghai Jikai Gene Chemistry Technology Co., Ltd.. According to the coding specificity of HOXA11-OS and miR-124-3p genes, the corresponding control sequences were obtained, and sh-HOXA11-OS and miR-124-3p inhibition sequences were designed according to the control sequences. And the sequences used in this study were shown as below: sh-NC: CCATGATTCCTTCATATTTGC; sh-HOXA11-OS: ACCGGCCGGCAAGGCTATGACATTTTCAAGAGAAATGTCA

TAGCCTTGCCGGTTTT; miR-124-3p inhibition: ACCGGGCATTCACCGCGTG

CCTTATTTT. The experimental mice were randomly divided into eight groups, each with six mice: 1) Control group: normal mice injected with negative control AAV; 2) sh-HOXA11-OS group: normal mice injected with knockdown HOXA11-OS AAV; 3) miR-124-3p inhibition group: normal mice injected with miR-124-3p inhibition AAV; 4) sh-HOXA11-OS+miR-124-3p inhibition group: normal mice injected with knockdown HOXA11-OS AAV and miR-124-3p inhibition AAV; 5) Lupus group: lupus mice injected with negative control AAV; 6) Lupus+sh-HOXA11-OS group: lupus mice injected with knockdown HOXA11-OS AAV; 7) Lupus+miR-124-3p inhibition group: lupus mice injected with miR-124-3p inhibition AAV; and 8) Lupus+sh-HOXA11-OS+miR-124-3p inhibition group: lupus mice injected with knockdown HOXA11-OS AAV and miR-124-3p inhibition AAV. The concentration of AAV was 5 x 10^{11} vg/ml, and the effects of AAV in all mice lasted for 1 month after in vivo injection.

Cell culture and model establishment

The mouse podocyte cell line MPC5, donated by Professor Lin Xu of Youjiang Medical College for Nationalities, was cultured in RPMI-1640 medium containing 10% fetal bovine serum (FBS) but not interferon-gamma in a cell incubator at 37 ℃ and 5% CO2. Lentivirus vectors were used to transfect podocytes to achieve overexpression and knockdown of the target genes. Stable cell lines were screened by puromycin(5μg/ml，48h) in culture medium. The lentivirus vector used in the experiment was designed and constructed by Shanghai Jikai Gene Chemistry Technology Co., Ltd.. According to the coding specificity of HOXA11-OS, miR-124-3p and Cyr61 genes, the corresponding control sequences were obtained, and ex-HOXA11-OS, sh-HOXA11-OS, miR-124-3p mimic, miR-124-3p inhibition and sh-Cyr61 sequences were designed according to the control sequences. And the sequences used in this study were shown as below: ex-HOXA11-OS，

GTCGGAGGAAGCGAGGTTTTCCGGGGTGCCGTAAGCCGTCTCGAAAAACTGGTCGAAAGCCTGTGGCAGAACGCCGTTCCTGCCCACCGTGCTATAGAAATTGGACGA
CGGGGGTGGGGTGGTGGTAGACGTTGGCCGAGCTCTTGGCCAGCACGTCGCCAGGCACGCCGGCCGCGCTGGGCGCCTGCAGACAGTCTCTGTGCACGAGCTCCTCC
GTAGCAGTGGGCCAGATTGCCGCGGGGGTGCCATTTAGTGGCGGGCTCAATGGCGTACTCTCTGAAGGTCACTTCGCGCACGGGTTGGACCTGGGGCAGGTTGGAGGA
GTATGTCATTGGGCGCGAAGACGGGGTCTGGGGCAAAAAAGAAGGGAGGCTGGAGAAATCTGGACCCGAGACGTAGTAAG
TACAACTTGGCAAATACATGTTAGAGGAGCAGGGACCACGCTCATCAAAATCCATCATTGGGCTACCTTGGGCTCTCCGCAGTAGCCGAGCTTAACATGATTCTCCACTG
CTGCCTCTTTGAAGCGGATCCGTGAAGTAGAAATTTGGAGACCCACCTCAGGGGAAGCAACAGATCGTCACTCGGTGTTCTCACCGAAAGCACGTAATCGCCGGTGTAA
CGCAGAAAGGCTGGGGTGCGCCCCCGGGCAGCTCTCCTTTGCTCAGCTACATGGTCCTGGTCCACGAGTGCTCTGAGGGCGGCAAGAGAGCGCAACTCCTGACGCCTC
GTTTGCTCTGGGAAGCCCCCCAGCCTCAGACCCTGGCTGGACCCCATTTGGGGCCAGGCTTCGCCGGCACGGATGTGCCGGCCTCGTGGCTTGTCCGATTTGCACGGT

CACTTCCGAAGCGCTTTAGTGCCTTCCGTCCCCAAACCGCCAACAGGCAAAGCGGCTTCCCTCCGCGGGGTTCGGAGTGACTCCTCAGAGCCAGAGGCACTTCTGCTCA
CTGAAGCTGACGAATCGGGAAACCATGCAATTGAGGCGAACCTTGGGCTGTTTTAGAGGCGCTGAGGAGCCTTCTCCTGGGAGGCCCAAGGTTGATTTCAGCCCACCAC
TAAGAGCACACCAAAAGGCCAAGTCCGAGTTCCATTTCTAGAAGAGGCGGCTTCCGGCAAGGCTATGACATTGGCCCTGGACATTGGTTTCCCAGGAGCTGCTTTTTCTC
AAAACGCTCTTCAACGTTTATTTCTTTTAATCGTCGCCCGGAGCCCTAAGGCGGCTAATGCAAGAGGCCAAAAATGTTT
GGAGGAAGAAAAACAAAGGCAGGAAGTGGCCGCGGCCTGACGGTGCGTGTGTGTCTGTAAAGAAGGGAGGGA
GCCGGTTCAACCTCCCCTCGTTTTCCCGAACTTCAAGGTCTAGGCAGACCCCCTTAGGGCCTTGCCGAGGCTCGCCCCCACACCCCCAGCGGCGCAGCATTTGGAGGTG
ATTTGATCGGCAGAACAAACCAACCCTTTTCGGAGGTTTCTTTTGATTTGGTCCTAAAGGGTATATGCTAGTGTCCACAGCGGCTGGGGTGGCTGCTGTTTTCCTCCCG
GATTCAGGCACCTTGCGCTGGCTGCACTCTCCTTCTGAGATAGAATACCAG[ex-NC:GGGTCAATATGTAATTTTCAG

TG; sh-HOXA11-OS#1: CCGGCCGGCAAGGCTATGACATTCTCGAGAATGTCA

TAGCCTTGCCGGTTTTT; sh-HOXA11-OS#2: CCGGGCTCTCCTTTGCTCAGCT

ACTCGAGTAGCTGAGCAAAGGAGAGCTTTTT; sh-HOXA11-OS#3: CCGGCC

ACCGTGCTATAGAAATTCTCGAGAATTTCTATAGCACGGTGGTTTTT; sh-NC: GGAAAGAATAGTAGACATAATAGC. sh-Cyr61#1: CCGGTTCCGACTGTACAG

CCTATTCCTCGAGGAATAGGCTGTACAGTCGGAATTTTT; sh-Cyr61#2: CCGG

TAACGAGAAACAATGAGTTAACTCGAGTTAACTCATTGTTTCTCGTTATTTTT; sh-Cyr61#3: CCGGCCTGTGAATATAACTCCAGAACTCGAGTTCTGGAGTTA

TATTCACAGGTTTTT; and its control sh-NC: CCATGATTCCTTCATATTTGC[miR-124-3p mimic: CTTCCTTCTTTCTTTCCTTCCTTCCTTCTTCCTTCCTCAG

GAGAAAGGCCTCTCTCTCCGTGTTCACAGCGGACCTTGATTTAAATGTCCATACAATTAAGGCACGCGGTGAATGCCAAGAATGGGGCTGTCTGAGCACCTTGGGTCCA
CAACGCCCTGGGCAGATCTCAGCGCTGCAGCTGCAGGCGCCCACAGTACTTTTTT; miR-124-

3p inhibition: CCGGGGCATTCACCGCGTGCCTTATTTTTG; miR-NC: CCATGA

TTCCTTCATATTTGC.

Extraction and determination of serum IgG concentration

Serum IgG was separated and purified by protein affinity chromatography column elution by washing, loading column, equilibrium, loading sample, washing, elution and neutralization. The concentration of IgG was determined according to the operation instructions of the kit.

CCK-8 assay

Podocytes were induced with different concentrations of lupus serum IgG (250, 500, or 1000 μg/mL) for 3, 6, and 12 h after incubation for 24 h. The supernatant formed after induction was discarded and 10 μL CCK-8 solution was added to each well. After incubation for about 1 h, the optical density (OD) at 450 nm was measured in a microplate reader.

Quantitative real time-polymerase chain reaction (qRT-PCR)

Total RNA was extracted in strict accordance with the instructions of the total RNA extraction kit. A reverse transcription kit was used to reverse transcribe RNA into complementary DNA. SYBR Green qPCR kit was used for qRT-PCR detection using three replicates. The two-step amplification procedure was adopted, and the reaction conditions were as follows: pre-denaturation at 95 ℃ for 30s, 1 cycle; Denaturation at 95 ℃ for 10s, annealing & extension at 60 ℃ for 30s, 40 cycles. The relative expression level of genes was calculated by using the 2-ΔΔCt formula. U6 was used as the internal reference for miR-124-3p and β-actin as the internal reference for other genes. The sequences of the primers used in this experiment are shown in Table 1.

Fluorescence in situ hybridization (FISH)

Cells fixed on slides were permeated with 0.5% Triton X-100 [0.1 M in phosphate-buffered saline (PBS)] for 10 min and then incubated in a pre-hybridization solution (without probe) on a climbing piece (floating method). Pre-hybridization was performed at 37 ℃ in a sealed wet box for 30 min-2 h. After rinsing, first at 42 ℃ and then at room temperature, 4′,6-diamidino-2-phenylindole (DAPI) was added dropwise and cells were incubated for 5 min,. Excess DAPI was removed by washing four times with PBS plus Tween 20 (PBST) for 5 min each time. A sealing sheet liquid containing an anti-fluorescence quencher was applied before fluorescence microscopy observation.

Double luciferase gene reporting assay

The binding sites of miR-124-3p to HOXA11-OS and Cyr61 were analyzed by bioinformatics. The activity of luciferase was determined using the double luciferase detection kit. The fragments of HOXA11-OS and Cyr61 bound to miR-124-3p were amplified by qRT-PCR, and then inserted into the pMIR-REPORT vector to construct wild-type (WT) plasmids of HOXA11-OS and Cyr61. The binding sites were then mutated by gene mutation technology to construct mutant (MUT) plasmids of HOXA11-OS and Cyr61. 293T cells were transfected with HOXA11-OS and Cyr61 WT or MUT plasmids and miR-124-3p mimics, either alone or in combination. After 24 h, luciferase activity was analyzed using the double luciferase reporter detection system.

Renal function measurement

Serum creatinine (Scr), urea nitrogen (BUN), and 24 h urine protein levels were analyzed to evaluate renal function using the Scr, BUN, and 24 h urine protein detection kits, respectively, following the manufacturers' instructions.

ELISA

The levels of Anti-dsDNA, ANA, and Anti-Sm antibodies in mice serum were detected using the respective ELISA kits. The absorbance was measured at 450 nm by a microplate reader.

Hematoxylin-eosin (HE) and periodate Schiff (PAS) staining

The kidney tissues of mice was fixed in 4% paraformaldehyde fixation solution, embedded with paraffin wax, and then sectioned continuously (approximately 4 μm in thickness). Dewax and hydration were performed before HE or PAS staining for optical microscopy analysis.

Western blotting

Mouse kidney tissue and podocytes were lysed in RIPA lysis solution and then centrifuged at 4 ℃ and 12,000 rpm for 5 min to collect the supernatant. Protein concentration was detected using the bicinchoninic acid assay. After sodium dodecyl-sulfate polyacrylamide gel electrophoresis, the denatured protein was transferred to a polyvinylidene difluoride membrane, which was sealed in Quick Block™ Western sealing solution at room temperature for 10 min. Cyr61(1:1500), Beclin-1(1:2000), LC3B(1:2000), nephrin(1:1500), podocin(1:2000), GAPDH(1:6000), and β-actin(1:6000) were then added and incubated overnight in a shaking table at 4 ℃. The membrane was reacted with horseradish peroxidase secondary antibody(1:20000), developed by ECL reagent, and measured using ImageJ 1.8.0 (National Institutes of Health, Bethesda, MD, USA) to calculate the expression of each protein.

Immunofluorescence (IF) assay

Podocytes(1×10^4 cells/well) were inoculated into confocal culture dishes for 24h and 4% paraformaldehyde cell fixation solution was added for 30 min. The cells were permeated with 0.1% TritonX-100-PBS for 20 min, and then sealed with 10% bovine serum albumin for 30 min. The primary antibodies of Cyr61(1:200), LC3B(1:800), nephrin(1:200) and tubulin(1:200) were added and incubated overnight at 4 ℃. After further incubation with fluorescent secondary antibody(1:200) in the dark for 1 h, 1~2 drops of DAPI were added for nuclear staining for 10 min, followed by anti-fluorescence quencher addition.

Mice kidney tissue sections were dewaxed by dimethylbenzene, dehydrated in a graded ethanol series, and boiled in ethylenediaminetetraacetic acid buffer (pH 8.0) for 20 min for antigen repair. For sealing, 10% bovine serum albumin was added for 1 h. Cyr61(1:200), LC3B(1:800), and nephrin(1:200) were then added and tissue sections were further incubated overnight; After incubation with fluorescent secondary antibody(1:200) for 1 h, 1~2 drops of DAPI were added for nuclear staining for 10 min, and the anti-fluorescent quenching tablets were sealed. The laser confocal microscope was used to analyze samples.

Statistical analyses

Data were analyzed in SPSS 23.0 (IBM, Armonk, NY, USA) and GraphPad Prism 8.0 (GraphPad Software, San Diego, CA, USA). All data are expressed as means ± standard deviation. The independent samples *t*-test was used for comparing two groups. One-way analysis of variance was used for comparing multiple groups, and the least significant difference test was used for comparing groups when variance was homogeneous. Tamhane's T^2 test was used when the variance was not uniform. $P < 0.05$ indicates statistical significance.

Results

Increased expression of HOXA11-OS, Cyr61, Beclin-1, and LC3B in the kidney tissue of lupus mice and serum of lupus patients

The expression levels of HOXA11-OS, Cyr61, and autophagy factors Beclin-1 and LC3B in the kidney tissue of lupus mice and serum of lupus patients were detected by qRT-PCR and western blotting. Compared with the control group, the expression levels of HOXA11-OS, Cyr61, Beclin-1, and LC3B were significantly enhanced ($P < 0.05$) (Fig. 1A).

Serum IgG from lupus patients induced the expression of HOXA11-OS, Cyr61, Beclin-1, and LC3B in podocytes in a concentration-dependent manner

To establish a cell model in vitro, podocytes were induced with different concentrations of serum IgG from lupus patients (LN-IgG 250, 500, or 1000 μg/mL) for 3, 6, and 12 h. The results showed that cell viability decreased gradually with increased induction time and dose, and the half inhibitory concentration appeared at induction using IgG 1000 μg/mL for 6 h (Fig. 1B). The results showed that LN-IgG could inhibit the activity of podocytes, and those induced at 1000 μg/mL LN-IgG for 6 h were used in the follow-up experiments.

According to the effects of LN-IgG on podocyte viability under the different conditions, we induced podocytes with different concentrations of LN-IgG for 6 h, and then collected them for qRT-PCR and western blot analyses. The expression levels of HOXA11-OS, Cyr61, Beclin-1, and LC3B were significantly increased, and the increase was most obvious when podocytes were induced by IgG at 1000 μg/mL for 6 h ($P < 0.05$) (Fig. 1C).

Subsequently, the effects of podocyte induction with LN-IgG or serum IgG for 6 h on the expression levels of Cyr61, Beclin-1, and LC3B were compared using the same method and different normal serum IgG concentrations (NC-IgG 250, 500, or 1000 μg/mL). There were no significant differences in the expression levels of Cyr61, Beclin-1, and LC3B ($P > 0.05$) between LN-IgG- and NC-IgG-induced groups (Fig. 1D). These results suggest that serum IgG of lupus patients may regulate the expression of Cyr61 and autophagy factors in podocytes.

HOXA11-OS regulated the expression of Cyr61, autophagy, and podocyte markers in podocytes

We successfully constructed HOXA11-OS overexpression and knockdown stable cell lines after lentivirus transfection of podocytes and verified HOXA11-OS expression level by qRT-PCR. The expression level of HOXA11-OS was significantly increased in the ex-HOXA11-OS group ($P < 0.001$), while HOXA11-OS#1 and #3 were significantly decreased in the sh-HOXA11-OS group. HOXA11-OS#1 decreased most significantly, and the knockdown effect was the most pronounced ($P < 0.001$). Hence, HOXA11-OS#1 was selected for further experiments (Fig. 2A).

The qRT-PCR and western blot analyses were also used to detect the expression levels of Cyr61, Beclin-1, LC3B, and podocyte markers nephrin and podocin. Compared with ex-NC, the expression levels of Cyr61, Beclin-1, and LC3B in the ex-HOXA11-OS group were significantly increased, while those of nephrin and podocin were significantly decreased ($P < 0.01$). Compared with sh-NC, the expression levels of Cyr61, Beclin-1, and LC3B in the sh-HOXA11-OS#1 group were significantly decreased, while those of nephrin and podocin were significantly increased ($P < 0.01$) (Fig. 2B).

In addition, the localization and expression of Cyr61, LC3B, and nephrin proteins were observed by IF. Cyr61, as a secretory protein, was expressed in the nucleus and cytoplasm, nephrin was expressed in the cell membrane, and LC3B was expressed in the cytoplasm. The expressions of Cyr61, LC3B, and nephrin obtained by IF were consistent with that obtained by western blotting (Fig. 2C). These results suggest that HOXA11-OS may affect podocyte function by regulating Cyr61 expression and autophagy.

miR-124-3p directly targeted the 3' untranslated region of HOXA11-OS and Cyr61 in podocytes

Firstly, the subcellular localization of HOXA11-OS was detected by FISH. The expressions of 18S, U6, and HOXA11-OS were similar, and there was no significant difference in OD ($P > 0.05$). HOXA11-OS was distributed in both the nucleus and cytoplasm but mainly in the cytoplasm (Fig. 3A). In addition, qRT-PCR results showed that miR-124-3p expression was low in both the kidney tissue of lupus mice and podocyte injury model, when compared with the control group ($P < 0.05$) (Fig. 3B). In the podocyte injury model, overexpression of HOXA11-OS significantly decreased the expression level of miR-124-3p, while HOXA11-OS knockdown significantly increased the expression level of miR-124-3p ($P < 0.001$). Furthermore, the overexpression of miR-124-3p significantly decreased the expression level of HOXA11-OS, while miR-124-3p knockdown significantly enhanced the expression level of HOXA11-OS ($P < 0.001$) (Fig. 3C). These results indicate that the expression level of HOXA11-OS is negatively correlated with that of miR-124-3p and that HOXA11-OS may regulate miR-124-3p by ceRNA.

Data in the Bibiserv database (https://bibiserv.cebitec.uni-bielefeld.de/rnahy Brid? ID = rnahybrid_view_submission) and Targetscan database (http://www.target-scan.org) predicted miR-124-3p targeted binding sites in both HOXA11-OS and Cyr61. The double luciferase reporter gene assay showed that the miR-124-3p mimic significantly reduced luciferase activity in cells transfected with the HOXA11-OS or Cyr61 WT reporter gene but had almost no inhibitory effect on cells transfected with HOXA11-OS or Cyr61 MUT reporter gene (Fig. 3D). In conclusion, miR-124-3p can bind directly to the predicted binding sites of HOXA11-OS and Cyr61.

HOXA11-OS mediated Cyr61 regulation of autophagy factors and cell damage by targeting miR-124-3p

The experiments described above showed that the expression level of miR-124-3p was opposite to that of HOXA11-OS and Cyr61, both containing direct targeting binding sites of miR-124-3p. This suggested that HOXA11-OS could mediate Cyr61 to regulate autophagy expression of podocytes by sponging miR-124-3p thereby affecting podocyte function. To validate this hypothesis, a miR-124-3p-overexpression lentivirus was transfected into the HOXA11-OS stable cell line. Cyr61 expression, levels of autophagy factors, and podocyte injury were detected by qRT-PCR and western blotting. The overexpression of Cyr61 and abnormally elevated levels of autophagy factors Beclin-1 and LC3B induced by HOXA11-OS overexpression were downregulated, the podocyte marker proteins nephrin and podocin were upregulated, and podocyte injury was alleviated by miR-124-3p overexpression ($P < 0.05$) (Fig. 4A). After transfection of miR-124-3p knockdown lentivirus into the constructed knockdown HOXA11-OS stable cell line, the low expression of Cyr61 and the decreased levels of Beclin-1 and LC3B due to HOXA11-OS knockdown were reversed to some extent, while nephrin and podocin were downregulated and podocyte injury was aggravated ($P < 0.05$) (Fig. 4B). In addition, we observed the localization and expression of Cyr61, LC3B, and nephrin proteins by IF. The localization of Cyr61, LC3B and nephrin proteins was the same as described above, and the proteins expression trend was consistent with that detected by western blotting (Fig. 4C-D).

Downregulation of Cyr61 can reverse the abnormal autophagy and podocyte injury induced by HOXA11-OS

In the present study, the expression of Cyr61 was downregulated by knocking down the lentivirus-transfected podocytes (Fig. 5A). The qRT-PCR and western blotting results revealed that the expression levels of HOXA11-OS, Cyr61, Beclin-1, and LC3B were significantly decreased, while nephrin and podocin were significantly increased in stable podocyte lines with downregulated Cyr61 (Fig. 5B). These results suggest that Cyr61 downregulation may reduce podocyte injury by downregulating the high expression of HOXA11-OS and reducing the abnormally elevated podocyte autophagy. Subsequently, the Cyr61 knockdown lentivirus was transfected into the constructed HOXA11-OS overexpressed stable cell line, and the expression level of the target gene was detected by qRT-PCR, western blot, and IF analyses. The results showed that the abnormal increase of autophagy caused by HOXA11-OS overexpression could be reversed to some extent, and the expression levels of Beclin-1 and LC3B decreased significantly, while that of nephrin and podocin increased significantly ($P < 0.05$); podocyte injury was alleviated (Fig. 5C-D). The recovery validation test showed that Cyr61 downregulation could alleviate the abnormally elevated autophagy of podocytes induced by the overexpression of HOXA11-OS and reduce podocytes damage.

miR-124-3p inhibition led to the deterioration of lupus mice with relieved injury after HOXA11-OS knockdown

To further verify the molecular mechanism of HOXA11-OS in the occurrence and development of LN in vivo, sh-HOXA11-OS and miR-124-3p inhibition AAVs were injected into mice kidneys, and changes in the renal function and autoantibody levels were detected. The levels of 24 h urinary protein, BUN, Scr, as well as anti-dsDNA, ANA, and anti-Sm antibodies in the Lupus + sh-HOXA11-OS group were significantly lower than those in the Lupus group ($P < 0.05$), while those in the Lupus + miR-124-3p inhibition group were significantly higher ($P < 0.05$). After treatment with both sh-HOXA11-OS and miR-124-3p inhibition AAV, the levels of 24 h urinary protein, BUN, Scr, as well as the levels of Anti-dsDNA, ANA, and Anti-Sm antibodies in mice were significantly higher than those in the Lupus + sh-HOXA11-OS group ($P < 0.05$) (Fig. 6A).

HE and PAS staining showed that compared with the control group, the glomeruli in the Lupus group showed contraction and deformation at different degrees, glomerular capillary stenosis and occlusion, mesangial cells and endothelial cells proliferated, and inflammatory cells were infiltrated in the renal interstitium. After injection of sh-HOXA11-OS AAV, pathological lesions in the kidney tissue of mice in the Lupus + sh-HOXA11-OS group were significantly improved compared with those of mice in the Lupus group; the morphology of glomeruli was relatively normal, there was no obvious stenosis and occlusion of glomerular capillaries, the proliferation of mesangial cells and endothelial cells was reduced, and infiltrated inflammatory cells were also decreased significantly. After injection of miR-124-3p inhibition AAV, the pathological lesions in the renal tissue of mice in the Lupus + sh-HOXA11-OS + miR-124-3p inhibition group were further aggravated compared to those of mice in the Lupus + sh-HOXA11-OS group. These results indicate that HOXA11-OS is involved in renal pathological processes and knocking down HOXA11-OS can alleviate renal injury in lupus mice; however, knocking down miR-124-3p may aggravate renal function injury in lupus mice by reversing the effect of HOXA11-OS knockdown (Fig. 6B).

Effect of HOXA11-OS on the expression of autophagy factors and podocyte markers in lupus mice renal tissue by targeting miR-124-3p regulating Cyr61

The knockdown level of HOXA11-OS in mouse kidney tissue was detected by qRT-PCR after in situ injection of AAV (Fig. 7A). Our results confirmed that HOXA11-OS is highly expressed in LN, and the expression level of HOXA11-OS can be downregulated by injecting AAV in vivo. The qRT-PCR and western blot analyses revealed that the expression levels of Cyr61, Beclin-1, and LC3B in lupus mice were significantly decreased ($P < 0.01$), while that of nephrin and podocin were significantly increased ($P < 0.05$) after HOXA11-OS knockdown compared with the control group, suggesting that renal inflammatory lesions were alleviated. The expression levels of Cyr61, Beclin-1, and LC3B were significantly increased ($P < 0.01$), while that of nephrin and podocin were significantly decreased ($P < 0.05$) after miR-124-3p expression was downregulated, suggesting that renal inflammatory lesions were aggravated. Compared with the Lupus + sh-HOXA11-OS group, the expression levels of Cyr61, Beclin-1, and LC3B in the kidney tissue of mice in the control group were significantly increased ($P < 0.05$), while nephrin and podocin expression levels were significantly decreased ($P < 0.01$), after knockdown HOXA11-OS and knockdown miR-124-3p AAVs were injected simultaneously, reversing the effect of HOXA11-OS knockdown and aggravating kidney damage (Fig. 7B-C). We further analyzed the protein expression levels of Cyr61, LC3B, and nephrin in mouse kidney tissue by IF, and found that results were consistent with those of western blotting (Fig. 7D). Our experiments further verified that HOXA11-OS can positively regulate the expression of Cyr61 and autophagy by targeting miR-124-3p thereby affecting the renal function of lupus mice.

Discussion

It is well known that LN is the most common complication of SLE[18]. Although the pathogenesis of LN is well understood, research on its treatment progress is still limited, and most patients end up with chronic kidney disease or end-stage renal disease[19]. Furthermore, research on the whole molecular mechanism of SLE and LN induction is still incomplete.

lncRNAs have been shown as key participants in various biological processes and structures. HOXA11-OS is a recently discovered lncRNA. Increasing studies have shown that abnormally expressed HOXA11-OS plays a key role in the occurrence and development of some diseases, and it can be used as a potential marker and therapeutic target for future disease prevention and treatment[21, 22]. For example, HOXA11-OS has regulatory effects on genes in oral squamous cell carcinoma, gastric cancer, prostate cancer, and various kidney diseases[23–26]. In the present study, we found that HOXA11-OS was highly expressed in kidney tissue, podocytes of lupus mice, and serum of lupus patients. The results of the podocyte function experiment showed that HOXA11-OS could promote the increase of autophagy factors and aggravate podocyte damage. In addition, knockdown of HOXA11-OS in vivo obviously reduced the expression of autophagy factors in the kidney tissue of lupus mice and alleviated kidney function damage. These results suggest that HOXA11-OS can regulate podocyte function and may play an important role in the pathogenesis of LN. There are several hypotheses on the biological functions of lncRNAs, including the ceRNA hypothesis, which has always been the focus of researchers' attention. According to this hypothesis, specific lncRNAs can up-regulate the expression of miRNA target genes by reducing the damage to microRNA activity[27–28]. In the present study, we confirmed that HOXA11-OS is mainly distributed in the cytoplasm (FISH results), suggesting that HOXA11-OS can play a sponge adsorption role. The miRNA miR-124-3p has attracted much research attention. We found that the expression of miR-124-3p and HOXA11-OS were negatively correlated, and they had mutual regulation, which indicated that HOXA11-OS could act as the ceRNA of miR-124-3p.

Autophagy is considered as a double-edged sword. Excessive and insufficient autophagy both participate in the physiological processes of cells[29, 30]. Autophagy has been proven to participate in the injury process of podocytes[31]. The degree of autophagy is different in injured podocytes for different diseases[32]. It has been shown[33] that the level of autophagy in kidney tissue and blood of LN patients is significantly upregulated, and podocytes are seriously damaged. Vitamin D can protect podocytes from damage in LN patients by regulating autophagy activity. Cyr61 is a secreted protein with many biological effects[34, 35]. Cyr61 often shows obvious high expression during the onset of SLE. However, the specific regulatory mechanism of Cyr61 in SLE is not fully understood. It was found that Cyr61 and autophagic factors were highly expressed in the kidney tissue of lupus mice and in the serum and podocytes

of lupus patients, which was similar to the expression trend of HOXA11-OS but opposite to that of miR-124-3p. Bioinformatics analysis showed that miR-124-3p could simultaneously target the 3' untranslated region of HOXA11-OS and Cyr61, which was confirmed by the double luciferase reporter gene assay. Subsequently, our in vitro experiments showed that HOXA11-OS can target miR-124-3p to regulate the expression of Cyr61 and autophagy factors through sponging, thus affecting the function of podocytes. In addition, in vivo experiments confirmed that the HOXA11-OS/miR-124-3p/Cyr61 regulatory network can play a role in LN, mainly in regulating the expression of autophagy factors and podocyte marker proteins in kidney tissue. However, the degree of autophagy was not discussed in depth in this study, and the related mechanism of clinical samples is lacking. We will complement this research in the future to further consolidate the significance and value of the present study.

Conclusions

In conclusion, HOXA11-OS can mediate the expression of Cyr61 through miR-124-3p sponging, thus regulating the expression of podocyte autophagy factors and affecting the podocyte and kidney injury levels in lupus mice. This indicates that HOXA11-OS may be a potential molecular marker in the diagnosis and treatment of LN.

Abbreviations

LN, Lupus nephritis

SLE, systemic lupus erythematosus

HOXA11-OS, opposite strand of homeobox A11

lncRNA, long non-coding RNA

miRNAs, micro RNAs

ceRNA, competitive endogenous RNA

Cyr61, cysteine rich 61

Beclin-1, programmed cell death-1

LC3, microtubule associated protein 1 light chain 3

IgG, immunoglobulin G

AAV, adeno-associated virus

ECL, enhanced chemiluminescence

GAPDH, glyceraldehyde 3-phosphate dehydrogenase

ELISA, enzyme-linked immunosorbent assay

CCK-8, cell counting kit-8

FBS, fetal bovine serum

OD, optical density

PBS, phosphate-buffered saline

DAPI, 4’,6-diamidino-2-phenylindole

PBST, PBS plus Tween 20

WT, wild-type

MUT, mutant

Scr, serum creatinine

BUN, urea nitrogen

dsDNA, double stranded DNA

ANA, antinuclear antibody

Sm, Smith

HE, hematoxylin-eosin

PAS, periodate Schiff

IF, immunofluorescence

Declarations

Ethics approval and consent to participate

Animal experiments were approved by the Ethics Committee of Youjiang Medical College for Nationalities (Approval No.: 2020043001), and all procedures were carried out according to the guidelines of the National Institute of Health.

Consent for publication

Not applicable

Availability of data and materials

All data generated or analysed during this study are included in this published article.

Competing interests

The authors declare that there are no conflicts of interest regarding the publication of the present manuscript.

Funding

The research was supported by the National Natural Science Foundation of China (Nos. 81860296), and the Innovation Project of Youjiang Medical University for Nationalities (No. YXCXJH2021001).

Authors' contributions

XP, SC, RS, SL carried out the experimental work, conceived the study, and participated in its design and coordination. XP and YY drafted the manuscript. All authors read and approved the final manuscript.

Acknowledgements

Not applicable.

References

1. Narváez J. Systemic lupus erythematosus 2020[J]. Med Clin (Barc). 2020;155(11):494–501.
2. Nishad R, Mukhi D, Singh AK, et al. Growth hormone induces mitotic catastrophe of glomerular podocytes and contributes to proteinuria[J]. Cell Death Dis. 2021;12(4):342.
3. Sakhi H, Moktefi A, Bouachi K, et al. Podocyte Injury in Lupus Nephritis[J]. J Clin Med. 2019;8(9):1340.
4. Tian Y, Guo H, Miao X, et al. Nestin protects podocyte from injury in lupus nephritis by mitophagy and oxidative stress[J]. Cell Death Dis. 2020;11(5):319.
5. Kravets I, Mallipattu SK. The Role of Podocytes and Podocyte-Associated Biomarkers in Diagnosis and Treatment of Diabetic Kidney Disease[J]. J Endocr Soc. 2020;4(4):bvaa029.
6. Wei C, Zhao L, Liang H, et al. Recent advances in unraveling the molecular mechanisms and functions of HOXA11AS in human cancers and other diseases (Review)[J]. Oncol Rep. 2020;43(6):1737–54.
7. Lu CW, Zhou DD, Xie T, et al. HOXA11 antisense long noncoding RNA (HOXA11-AS): A promising lncRNA in human cancers[J]. Cancer Med. 2018;7(8):3792–9.
8. Zhao Z, Sun W, Guo Z, et al. Mechanisms of lncRNA/microRNA interactions in angiogenesis[J]. Life Sci. 2020;254:116900.
9. You L, Wu Q, Xin Z, et al. The long non-coding RNA HOXA11-AS activates ITGB3 expression to promote the migration and invasion of gastric cancer by sponging miR-124-3p[J]. Cancer Cell Int. 2021;21(1):576.
10. Liu H, Zhao L, Zhang J, et al. Critical Role of Cysteine-Rich Protein 61 in Mediating the Activation of Renal Fibroblasts[J]. Front Physiol. 2019;10:464.
11. Lin J, Li N, Chen H, et al. Serum Cyr61 is associated with clinical disease activity and inflammation in patients with systemic lupus erythematosus[J]. Med (Baltim). 2015;94(19):e834.
12. Guo P, Ma Y, Deng G, et al. CYR61, regulated by miR-22-3p and MALAT1, promotes autophagy in HK-2 cell inflammatory model[J]. Transl Androl Urol. 2021;10(8):3486–500.
13. Ichimiya T, Yamakawa T, Hirano T, et al. Autophagy and Autophagy-Related Diseases: A Review[J]. Int J Mol Sci. 2020;21(23):8974.
14. Vishnupriya S, Priya Dharshini LC, Sakthivel KM, et al. Autophagy markers as mediators of lung injury-implication for therapeutic intervention[J]. Life Sci. 2020;260:118308.

15. Koustas E, Sarantis P, Theoharis S, et al. Autophagy-related Proteins as a Prognostic Factor of Patients With Colorectal Cancer[J]. Am J Clin Oncol. 2019;42(10):767–76.
16. Zhou XJ, Klionsky DJ, Zhang H. Podocytes and autophagy: a potential therapeutic target in lupus nephritis[J]. Autophagy. 2019;15(5):908–12.
17. Jin J, Tu Q, Gong J, et al. Autophagy activity and expression pattern of autophagy-related markers in the podocytes of patients with lupus nephritis: association with pathological classification[J]. Ren Fail. 2019;41(1):294–302.
18. Kiriakidou M, Ching CL. Systemic Lupus Erythematosus[J]. Ann Intern Med. 2020;172(11):ITC81–96.
19. Parikh SV, Almaani S, Brodsky S, et al. Update on Lupus Nephritis: Core Curriculum 2020[J]. Am J Kidney Dis. 2020;76(2):265–81.
20. Lu S, Jiang X, Su Z, et al. The role of the long non-coding RNA HOXA11-AS in promoting proliferation and metastasis of malignant tumors[J]. Cell Biol Int. 2018;42(12):1596–601.
21. Xue JY, Huang C, Wang W, et al. HOXA11-AS: a novel regulator in human cancer proliferation and metastasis[J]. Onco Targets Ther. 2018;11:4387–93.
22. Lin FJ, Lin XD, Xu LY, et al. Long Noncoding RNA HOXA11-AS Modulates the Resistance of Nasopharyngeal Carcinoma Cells to Cisplatin via miR-454-3p/c-Met[J]. Mol Cells. 2020;43(10):856–69.
23. Niu X, Yang B, Liu F, et al. LncRNA HOXA11-AS promotes OSCC progression by sponging miR-98-5p to upregulate YBX2 expression[J]. Biomed Pharmacother. 2020;121:109623.
24. Liu Y, Zhang YM, Ma FB, et al. Long noncoding RNA HOXA11-AS promotes gastric cancer cell proliferation and invasion via SRSF1 and functions as a biomarker in gastric cancer[J]. World J Gastroenterol. 2019;25(22):2763–75.
25. Cheng Y, Xiong HY, Li YM, et al. LncRNA HOXA11-AS promotes cell growth by sponging miR-24-3p to regulate JPT1 in prostate cancer[J]. Eur Rev Med Pharmacol Sci. 2021;25(14):4668–77.
26. Zhu S, Zhang J, Cui Y, et al. Long non-coding RNA HOXA11-AS upregulates Cyclin D2 to inhibit apoptosis and promote cell cycle progression in nephroblastoma by recruiting forkhead box P2[J]. Am J Cancer Res. 2020;10(1):284–98.
27. Zhang P, Wu W, Chen Q, et al. Non-Coding RNAs and their Integrated Networks[J]. J Integr Bioinform. 2019;16(3):20190027.
28. Xu CH, Xiao LM, Liu Y, et al. The lncRNA HOXA11-AS promotes glioma cell growth and metastasis by targeting miR-130a-5p/HMGB2[J]. Eur Rev Med Pharmacol Sci. 2019;23(1):241–52.
29. Allen EA, Baehrecke EH. Autophagy in animal development[J]. Cell Death Differ. 2020;27(3):903–18.
30. Chang NC. Autophagy and Stem Cells: Self-Eating for Self-Renewal[J]. Front Cell Dev Biol. 2020;8:138.
31. Qi YY, Zhou XJ, Cheng FJ, et al. Increased autophagy is cytoprotective against podocyte injury induced by antibody and interferon-α in lupus nephritis[J]. Ann Rheum Dis. 2018;77(12):1799–809.
32. Xu J, Deng Y, Wang Y, et al. SPAG5-AS1 inhibited autophagy and aggravated apoptosis of podocytes via SPAG5/AKT/mTOR pathway[J]. Cell Prolif. 2020;53(2):e12738.
33. Yu Q, Qiao Y, Liu D, et al. Vitamin D protects podocytes from autoantibodies induced injury in lupus nephritis by reducing aberrant autophagy[J]. Arthritis Res Ther. 2019;21(1):19.
34. Bartkowiak K, Heidrich I, Kwiatkowski M, et al. Cysteine-Rich Angiogenic Inducer 61: Pro-Survival Function and Role as a Biomarker for Disseminating Breast Cancer Cells[J]. Cancers (Basel). 2021;13(3):563.
35. Fan Y, Yang X, Zhao J, et al. Cysteine-rich 61 (Cyr61): a biomarker reflecting disease activity in rheumatoid arthritis[J]. Arthritis Res Ther. 2019;21(1):123.

Tables

Table 1 is available in the Supplementary Files section.

Figures

Figure 1

HOXA11-OS, Cyr61, Beclin-1, and LC3B are highly expressed in kidney tissue, serum, and cell lines of LN. **A** Expression levels of HOXA11-OS, Cyr61, Beclin-1, and LC3B in the kidney tissue of lupus mice and serum of lupus patients as detected by qRT-PCR and western blotting. $^{*}P < 0.05$ vs. control group. Data represent means ± standard deviation. **B** Different concentrations of serum IgG (250, 500, or 1000 μg/mL) in lupus patients induced podocytes for 3, 6, and 12 h. Podocyte activity was detected by CCK-8. $^{*}P < 0.05$ vs. 0 μg/mL; $^{\#}P < 0.05$ vs. 3 h. **C** Expression levels of HOXA11-OS, Cyr61, Beclin-1, and LC3B as detected by qRT-PCR and western blotting after podocytes were induced by different concentrations of IgG in lupus patients sera for 6 h. $^{*}P < 0.05$ vs. control group. **D** Expression levels of Cyr61, Beclin-1, and LC3B as detected by qRT-PCR and western blot after podocytes were induced by different concentrations of IgG in normal human serum for 6 h. The expression levels of Cyr61, Beclin-1, and LC3B were not significantly different

Figure 2

Expression levels of Cyr61, autophagy factors, and podocyte markers in podocytes regulated by HOXA11-OS. **A** HOXA11-OS mRNA expression levels were detected by qRT-PCR after HOXA11-OS overexpression and knockdown lentivirus were successfully transfected into podocytes. $^{*}P < 0.001$ vs. ex-NC; $^{*}P < 0.001$ vs. sh-NC. **B** After HOXA11-OS overexpression and knockdown lentivirus were successfully transfected into podocytes, the expression levels of Cyr61, Beclin-1, LC3B, nephrin, and podocin were detected by qRT-PCR and western blotting. $^{*}P < 0.01$ vs. ex-NC; $^{\#}P < 0.01$ vs. sh-NC. **C** After HOXA11-OS overexpression and knockdown lentivirus were successfully transfected into podocytes, the localization and expression levels of Cyr61, LC3B, and nephrin proteins in each group were detected by IF. Relative average OD: $^{*}P < 0.01$ vs. ex-NC; $^{\#}P < 0.01$ vs. sh-NC. Scale bars represent 15 μm

Figure 3

miR-124-3p directly binds to the 3' untranslated regions of HOXA11-OS and Cyr61 in podocytes. **A** The subcellular localization of HOXA11-OS was detected by FISH assay. The expression levels of 18S, U6, and HOXA11-OS were similar, and there was no statistical difference in OD. **B** The expression levels of miR-124-3p in the kidney tissue of lupus mice and podocyte injury model were detected by qRT-PCR. $^{*}P < 0.01$ vs. control group. **C** The expression levels of HOXA11-OS in miR-124-3p mimic or inhibition cell lines and the expression levels of miR-124-3p in HOXA11-OS overexpression or knockdown cell lines were detected by qRT-PCR. $^{*}P < 0.001$ vs. miR-NC/ex-NC/sh-NC. **D** The binding sites of miR-124-3p on HOXA11-OS and Cyr61 in HOXA11-OS-WT and Cyr61-WT, and the mutation sites in HOXA11-OS-MUT and Cyr61-MUT are indicated in red. Bi-luciferase reporter genes were detected 48 h after transfection of HOXA11-OS-WT, Cyr61-WT, HOXA11-OS-MUT, or Cyr61-MUT and miR-124-3p mimic or miR-NC. $^{**}P < 0.01$ vs. HOXA11-OS-WT+ miR-NC/Cyr61-WT + miR-NC

Figure 4

HOXA11-OS regulates autophagy factors and cell damage by targeting miR-124-3p mediated Cyr61. **A** The expression levels of Cyr61, Beclin-1, LC3B, nephrin, and podocin were detected by qRT-PCR and western blotting after transfection of miR-124-3p mimic into the ex-HOXA11-OS cell line. **B** The expression levels of Cyr61, Beclin-1, LC3B, nephrin, and podocin were detected by qRT-PCR and western blotting after transfection of miR-124-3p inhibition into the sh-HOXA11-OS#1 cell line. **C, D** The localization and expression levels of Cyr61, LC3B, and nephrin were detected by IF. $^{*}P < 0.05$ vs. miR-NC; $^{\#}P < 0.05$ vs. ex-HOXA11-OS+miR-NC/sh-HOXA11-OS#1+miR-NC. Data are means ± standard deviation. Scale bars represent 15 μm

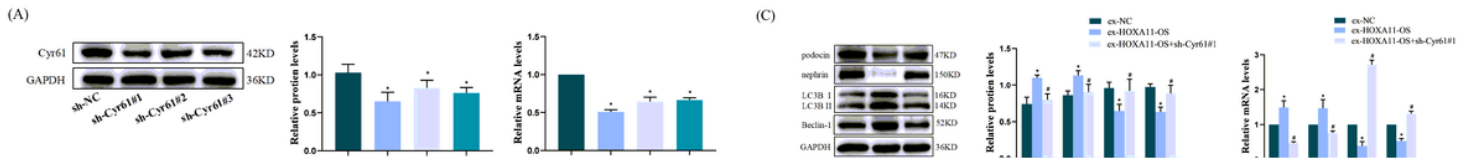

Figure 5

The downregulation of Cyr61 gene can reverse the abnormal autophagy and podocyte injury induced by HOXA11-OS. **A** The Cyr61 gene was downregulated by knockdown lentivirus transfected to podocytes, and its expression level was detected by qRT-PCR and western blotting. **B** The expression levels of HOXA11-OS, Beclin-1, LC3B, nephrin, and podocin were detected by qRT-PCR and western blotting after Cyr61 downregulation. $^{*}P < 0.05$ vs. sh-NC. **C** The expression levels of Beclin-1, LC3B, nephrin, and podocin were detected by qRT-PCR and western blotting after sh-Cyr61#1 was transfected into the ex-HOXA11-OS cell line. **D** The localization and expression levels of LC3B and nephrin were detected by IF. $^{*}P < 0.05$ vs. ex-NC; $^{\#}P < 0.05$ vs. ex-HOXA11-OS. Data are means ± standard deviation. Scale bars represent 15 μm

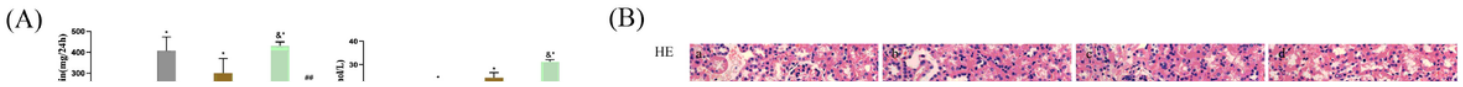

Figure 6

miR-124-3p inhibition led to the deterioration of lupus mice but podocyte injury was alleviated after HOXA11-OS knockdown. **A** 24 h urinary protein, BUN, Scr, and autoantibody levels of mice in each group. $^{\&}P > 0.05$, $^{*}P < 0.05$ vs. sh-NC; $^{\#}P < 0.05$ vs. sh-HOXA11-OS; $^{\&*}P < 0.05$ vs. Lupus+sh-NC; $^{\#\#}P < 0.05$ vs. Lupus+sh-HOXA11-OS. **B** HE and PAS staining of kidney tissue: (a) sh-NC; (b) sh-HOXA11-OS; (c) miR-124-3p inhibition; (d) sh-HOXA11-OS+miR-124-3p inhibition; (e) Lupus+sh-NC; (f) Lupus+sh-HOXA11-OS; (g) Lupus+miR-124-3p inhibition; (h) Lupus+sh-HOXA11-OS+miR-124-3p inhibition. Scale bars represent 20 μm

Figure 7

Effect of HOXA11-OS on the expression of autophagy factors and podocyte markers in kidney tissue by targeting miR-124-3p regulating Cyr61. **A** The expression of HOXA11-OS mRNA was detected by qRT-PCR after AAV was injected into mice kidney tissues. **B** The expression levels of Cyr61, Beclin-1, LC3B, nephrin, and podocin in kidney tissues of mice were detected by qRT-PCR and western blotting. **C** The expression levels of Cyr61, LC3B, and nephrin in kidney tissues of mice were detected by IF. $^{\&}P > 0.05$, $^{*}P < 0.05$ vs. sh-NC; $^{\#}P < 0.05$ vs. sh-HOXA11-OS; $^{\&*}P < 0.05$ vs. Lupus+sh-NC; $^{\#\#}P < 0.05$ vs. Lupus+sh-HOXA11-OS. Data are means ± standard deviation. Scale bars represent 15 μm

Supplementary Files

This is a list of supplementary files associated with this preprint. Click to download.

- Table1Primersequences.pdf